CONF-951203--45

Analysis of Radiation Measurement Data of the BUSS Cask*

Y. Y. Liu[1] and J. S. Tang[2]

[1]Argonne National Laboratory, Argonne, Illinois, USA
[2]Oak Ridge National Laboratory, Oak Ridge, Tennessee, USA

INTRODUCTION

The Beneficial Uses Shipping System (BUSS) is a Type-B packaging developed for shipping nonfissile, special-form radioactive materials to facilities such as sewage, food, and medical-product irradiators (Yoshimura et al. 1986). Radionuclides to be shipped in the BUSS cask are primarily ^{137}Cs in the form of doubly encapsulated cesium chloride (CsCl), or ^{90}Sr in the form of doubly encapsulated strontium fluoride (SrF_2). The primary purpose of the BUSS cask is to provide shielding and confinement, as well as impact, puncture, and thermal protection for its certified special-form contents under both normal transport and hypothetical accident conditions.

A BUSS cask that contained 16 CsCl capsules (2.723×10^4 TBq total activity) was recently subjected to radiation survey measurements at a Westinghouse Hanford facility, which provided data that could be used to validate computer codes. Two shielding analysis codes, MICROSHIELD (User's Manual 1988) and SAS4 (Tang 1993), that are used at Argonne National Laboratory to evaluate the safety of packaging of radioactive materials during transportation, have been selected for analysis of radiation data obtained from the BUSS cask. MICROSHIELD, which performs only gamma radiation shielding calculation, is based on a point-kernel model with idealized geometry, whereas SAS4 is a control module in the SCALE code system (1995) that can perform three-dimensional Monte Carlo shielding calculation for photons and neutrons, with built-in procedures for cross-section data processing and automated variance reduction. The two codes differ in how they model the details of the physics of gamma photon attenuation in materials, and this difference is reflected in the associated engineering cost of the analysis. One purpose of the analysis presented in this paper, therefore, is to examine the effects of the major modeling assumptions in the two codes on calculated dose rates, and to use the measured dose rates for comparison. The focus in this paper is on analysis of radiation dose rates measured on the general body of the cask and away from penetrations. A separate study of gamma radiation streaming from cask penetrations is also being conducted with three-dimensional Monte Carlo codes MORSE-SGC/S and MCNP4A; the results of that study will be reported elsewhere (Liu et al. 1996).

---

*This work was supported by the U.S. Department of Energy, Office of Facility Safety Analysis, under Contract W-31-109-Eng-38.

RADIATION MEASUREMENTS

A detailed description of the BUSS cask is given in the BUSS Cask Safety Analysis Report (1991) and will not be repeated here. Figure 1 is a schematic diagram of the BUSS cask, showing a cutaway view of the central cavity of the Type 304 stainless steel (304SS) cask body, the diametrically opposed upper and lower drain ports, the bolted lid, and the fins on the external surface of the cask. Not shown in the upper and lower drain ports in Fig. 1 are a bore plug, a valve assembly, drain plugs, and thermal covers, which facilitate drainage, gas filling, and reduction of radiation streaming. When the cask was loaded for radiation survey measurement at the Westinghouse facility, each of the sixteen 52.8-cm-long CsCl capsules was placed in a hole of the 304SS basket (Fig. 2) so that it would protrude 7.3 cm above the basket. After the loaded basket was lowered into the cask cavity, the 304SS lid was placed over the top of the basket before radiation was surveyed at various locations on the external surface of the cask, with and without inserting the lid bolts. Table 1 gives the measured dose rates for five cask configurations. Away from the upper and lower drain ports and the lid bolt holes without the bolts, the measured dose rates were relatively low, 0.16 and 0.05 mSv/h, respectively, at the top and cylindrical surfaces of the cask, irrespective of the measurement configurations. The estimated uncertainty of the measured dose rates is ±15% (Robins 1994).

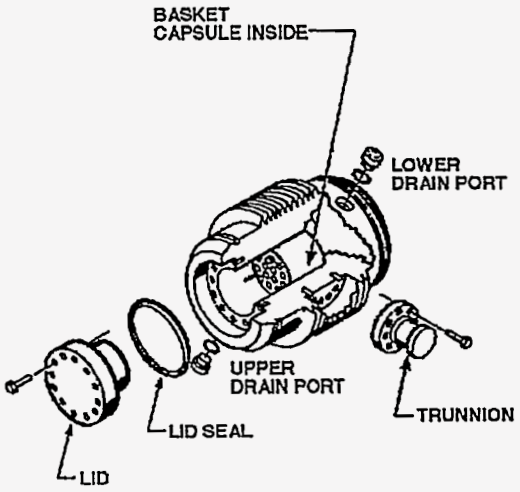

Figure 1. Schematic diagram of BUSS cask showing a cutaway view of cask body

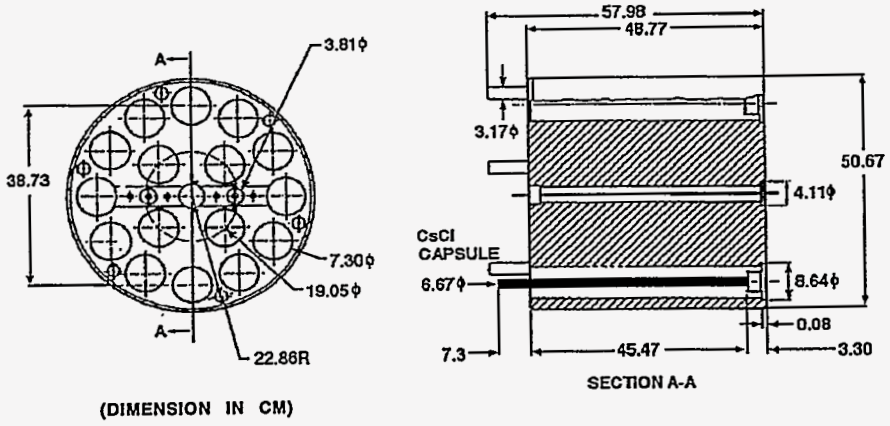

Figure 2. Sixteen hole Type 304 stainless steel basket used for CsCl capsules

Table 1. Radiation Survey Measurements (10^{-2} mSv/h) of the BUSS Cask Loaded with CsCl Capsules (Robins 1994)

Location	Configuration 1[a]	2[b]	3[c]	4[d]	5[e]
Upper Drain Port	700	500	450	15	7
Lower Drain Port	70	25	25	25	25
Lid Bolt Holes					
w/o Bolts	275	-	-	-	-
w/ Bolts	-	16	16	16	16
General Body	5	5	5	5	5

[a]Lid was seated on extended lid jacking screws. Lid bolts were not inserted. Drain plugs and thermal covers for upper and lower drain ports were not installed. A port valve assembly was installed for lower drain port and remained there during entire radiation survey measurements.

[b]Lid was seated on extended lid jacking screws. Lid bolts were inserted. Drain plugs were installed for upper and lower drain ports. Thermal covers were not installed for upper and lower drain ports.

[c]Lid was seated on lid seal with jacking screws retracted. Lid bolts were inserted. Drain plugs were installed for upper and lower drain ports. Thermal covers were not installed for upper and lower drain ports.

[d]Lid was seated on lid seal with jacking screws retracted. Lid bolts were inserted. A prototype bore plug was inserted in upper drain port. Drain plugs were installed for upper and lower drain ports. Thermal covers were not installed for upper and lower drain ports.

[e]Lid was seated on lid seal with jacking screws retracted. Lid bolts were inserted. A prototype bore plug was inserted in upper drain port. Drain plugs were installed for upper and lower drain ports. Thermal cover was installed for upper drain port. Thermal cover was not installed for lower drain port.

MICROSHIELD ANALYSIS

A simplified schematic diagram of the BUSS cask cross section that ignores the fins on the cylindrical surface is shown in Fig. 3, which also gives the dimensions and relative positions of the major components. To calculate radial and axial dose rates on the surface of the cask, two source-shield geometrical models in MICROSHIELD were used: a cylinder source with cylindrical shields (Fig. 4a) for the radial calculation, and a cylinder source with slab-end shields (Fig. 4b) for the axial calculation. In both models, the CsCl capsules were treated as an homogenized source uniformly distributed in a volume equivalent to that of the 304SS basket, ignoring the fact that portions of the CsCl capsules protrude above the basket. The source energy spectrum was taken to be 662 keV, the dominant peak of ^{137}Cs. Other pertinent properties (such as atomic densities, mass attenuation coefficients, etc.) of nuclides and shielding materials that were needed for the calculations were default values in MICROSHIELD; the only major modeling option exercised was the formula for calculating the buildup factor that accounts for forward scattering of photons in the shielding materials. The options were no buildup or buildup factor equal to unity, the Taylor formula, and the geometric progression (GP) formula, assuming in each case that the 304SS cask body and the lid were the dominant shields between the CsCl source and the detector.

Table 2 lists the inputs for the two MICROSHIELD source-shield models, the calculated and measured dose rates at four point-detector locations, A, B, C, and D, on the surface of

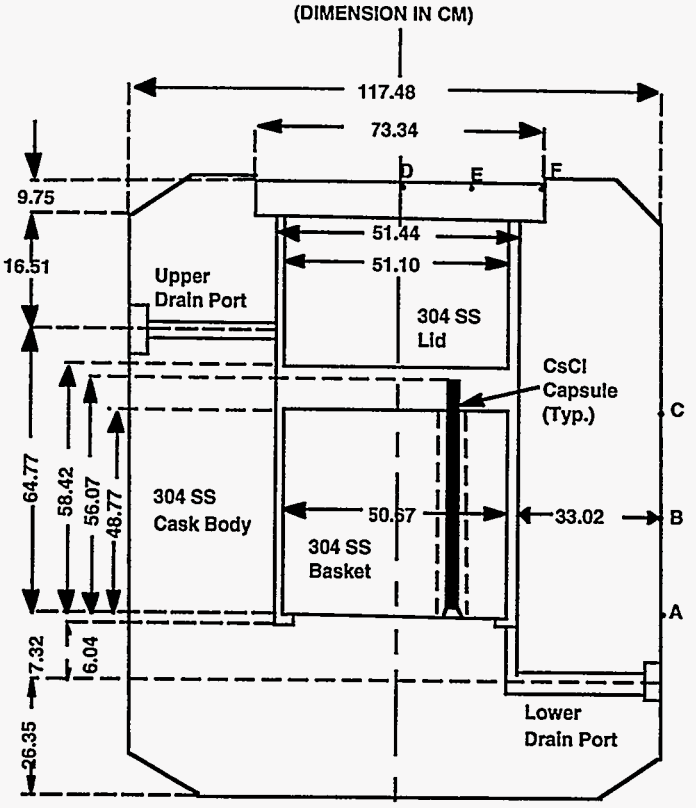

Figure 3. Schematic diagram of BUSS cask showing dimensions and relative positions of major components

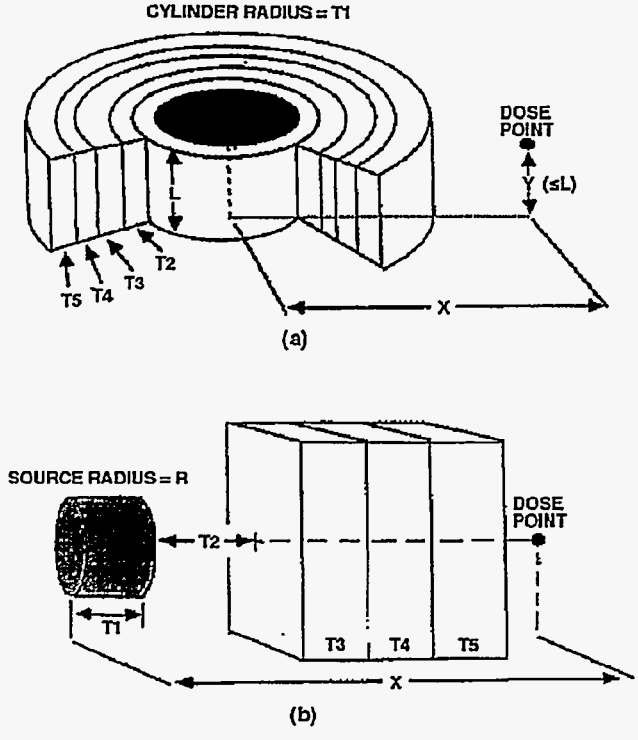

Figure 4. MICROSHIELD models used in radial and axial dose rate calculations: (a) cylinder-source/ cylindrical-shields model, and (b) cylinder-source/slab-end-shields model

the cask. When the forward scattering of photons in the shielding materials was ignored (i.e., with no buildup), the calculated dose rates are all much smaller than the measured dose rates. The dose rates (1.8-3.2 x 10^{-2} mSv/h) calculated by the cylinder-source/ cylindrical-shields model at locations A, B, and C on the cylindrical surface of the cask are somewhat lower than the measured dose rate of 5 x 10^{-2} mSv/h, which could be explained by the fact that the MICROSHIELD model did not consider those portions of the CsCl capsules protruding above the basket, and thus underestimated the actual gamma radiation particularly for location C near the top of the basket. For similar reasons, the dose rates (10.1-10.2 x 10^{-2} mSv/h) calculated by the cylinder-source/slab-end-shields model at location D on the lid surface of the cask are also lower than the measured value of 16 x 10^{-2} mSv/h. Generally, the Taylor formula gave slightly higher dose rates than the GP formula, but the two sets of calculated dose rates at the four point-detector locations are too close to reveal any significant difference between the two buildup formulae. Another point to be noted in Table 2 is that in the cylinder-source/cylindrical-shields model, regardless of the buildup formula, the calculated dose rates were identical at detector locations A and C on the cask surface. This is apparently due to symmetry, and verifies the point-kernel numerical integration algorithm for the cylinder-source/cylindrical-shields model in MICROSHIELD.

Table 2. MICROSHIELD Inputs and Calculated and Measured Dose Rates on Cask Surface

	Point Detector Location[a]			
Parameters[b]	A	B	C	D
Source Activity (10^4 TBq)	2.723	2.723	2.723	2.723
T1 (cm), CsCl	25.34	25.34	25.34	45.47
T2 (cm), Air	0.38	0.38	0.38	9.65
T3 (cm), 304SS	33.02	33.02	33.02	32.61
L or R (cm), Source Length or Radius	45.47(L)	45.47(L)	45.47(L)	25.36(R)
X/Y (cm), Detector Location	58.74(X)	58.74(X)	58.74(X)	87.73(X)
	0.0(Y)	22.74(Y)	45.47(Y)	-
Dose Rate (10^{-2} mSv/h)[c]				
No Buildup	3.37 x 10^{-2}	3.90 x 10^{-2}	3.37 x 10^{-2}	0.20
Taylor	1.82	3.19	1.82	10.06
GP	1.80	3.15	1.80	10.16
Measured	5.0[d]	5.0[d]	5.0[d]	16.0

[a] A, B, C, and D are point detector locations defined in Fig. 3. A, B, and C are detector locations in cylinder-source/cylindrical-shields model in Fig. 4a, whereas D is detector location in cylinder-source/slab-end-shields model in Fig. 4b.

[b] The symbols (T1, T2, T3, L, R, X, and Y) in the table correspond directly to those defined in Fig. 4, and their values were based on dimensions in Fig. 3.

[c] Dose rates were calculated under assumptions that forward scattering of photons was modeled by three buildup formulae: no buildup (or buildup factor = 1), Taylor formula, and GP formula.

[d] Measured dose rates are assumed to be the same for locations A, B, and C.

SAS4 ANALYSIS

In the SAS4 analysis, the three-dimensional geometry of the BUSS cask was modeled in detail and each of the 16 CsCl capsules was represented as a discrete source in a hole of the 304SS basket. The geometry input, while taking advantage of the capability of the MARS combinatorial geometry (West and Emmett 1995), is quite laborious. However, SAS4 includes several major features that greatly simplified the present analysis task. Among the helpful features in SAS4 are the automated processing of several functional modules (BONAMI, NITAWL, XSDRNPM, and MORSE-SGC) in the SCALE code system (1995) for resonance self-shielding calculations, cell-weighted cross sections, and adjoint flux calculations to generate the biasing parameters that were subsequently used in the Monte Carlo calculations of photon transport from the discrete CsCl sources through the basket, wall, and/or lid of the cask. For variance reduction in the Monte Carlo calculations, SAS4 also automatically invoked all of the standard biasing techniques (e.g., source biasing, subparticle splitting and Russian Roulette, particle path-length stretching, and collision energy biasing) in MORSE-SGC so that the user was spared the burden of a rather difficult task.

To describe the CsCl photon source, the line spectrum of 662 keV was specified in the SAS4 source-energy spectrum array (between 600 and 800 keV), which contains 27 neutron and 18 gamma energy groups based on the selection of the ENDF-B/IV 27n-18γ cross-section library. Other properties of nuclides and shielding materials needed for the calculations were default values in SAS4; the only modeling parameter that was varied was the number of histories required to generate reasonable statistics in the Monte Carlo calculations. With the number of source particles fixed at 3,000 per batch, the highest particle-history number was 600,000, which required ~20 minutes of CPU time on an R/6000 Model 390 workstation.

Table 3 lists radial and axial dose rates that were calculated for the surface of the cask, and their associated standard deviations (σ). Each set of dose rates was calculated at a surface detector and at three point-detector locations. The surface detectors at the cylindrical and lid surface of the cask have a finite dimension of a shell and a disk, respectively, whereas each of the six point detectors at locations A, B, C, D, E, and F (shown in Fig. 3) was located slightly away from the cask surface to avoid a $1/r^2$ singularity. Because of the nature of the boundary-crossing estimates for the escaped photon fluxes, the dose rates calculated for the two surface detectors are generally more reliable than those calculated for any of the point detectors, as illustrated in Table 3 by the much lower associated standard deviations. When compared with the measured dose rates (5 and 16 x 10^{-2} mSv/h) at the cylindrical and lid surfaces of the cask, the calculated total response dose rates (11.4 and 33.7 x 10^{-2} mSv/h) for the two surface detectors in the radial and axial calculations, respectively, are higher and the discrepancy could be due to the uncertainty in the exact locations where the measurements were taken. The total response dose rates calculated at the six point detector locations indicate that the dose rate is quite sensitive to the detector location relative to the portion of the source above the basket. For the radial case, the calculated dose rates vary by a factor of ~6, depending on the axial location. For the axial case, the calculated dose rates vary by almost a factor of 8, depending on the radial location. The calculated point-detector dose rates indeed follow the trend that is expected from shielding and geometry considerations, i.e., the additional shielding provided by the 304SS basket and the increased distance from source to detector resulted in the lowest calculated dose rate at point-detector location A, whereas the higher calculated dose rates at point-detector locations C, D and E resulted from treating the protruding portions of the CsCl capsules explicitly in the Monte Carlo calculations. Finally, Table 3 shows that the uncollided dose rates calculated for the point detectors (assuming no scattering of photons in the shielding

materials) are typically 2-3 orders of magnitude lower than the corresponding total response dose rates, thus underscoring the importance of modeling the physics of photon scattering in the Monte Carlo calculations.

Table 3. SAS4 Calculated and Measured Dose Rates (10^{-2} mSv/h) on Cask Surface[a]

Parameter	Uncollided (x 10^{-5})	σ_u[b] (%)	Total Response	σ_t[b] (%)
Radial Calculation				
Surface Detector on Cylindrical surface	0.0	0.0	11.4	1.9
Point Detectors				
A	3.5	25.8	3.4	16.9
B	12.3	15.3	8.5	12.7
C	34.3	18.3	19.5	15.0
Measured	-	-	5.0	15.0
Axial Calculation				
Surface Detector on Top of Lid	0.0	0.0	33.7	1.7
Point Detectors				
D	103.7	10.4	67.1	8.4
E	72.1	12.2	56.0	10.0
F	10.5	19.1	7.9	17.7
Measured	-	-	16.0	15.0

[a]A, B, C, D, E, and F are point detector locations defined in Fig. 3.

[b]σ_u and σ_t are associated standard deviations computed for uncollided and total response dose rates, respectively.

SUMMARY

Gamma radiation survey measurement data of the BUSS cask were analyzed with the MICROSHIELD code and the SAS4 control module in the SCALE code system. By treating CsCl capsules as uniformly distributed sources in cylindrical shields and slab-end shields models, the point-kernel calculations of MICROSHIELD underestimated the dose rates measured on the general body of the cask and away from penetrations. The calculated dose rates were not particularly sensitive to either of the two buildup formulae chosen for the dominant shield. Ease of use and fast turnaround are advantages that make MICROSHIELD a useful scoping analysis tool for the evaluation of gamma radiation shielding of transportation and storage casks. However, caution must be exercised when using approximate model of the source or the shielding material.

The SAS4 three-dimensional Monte Carlo dose rate calculations at the two surface detector locations were higher than the measured dose rates that could be due to the uncertainty in

the exact measurement locations on the cask. The calculated dose rates at the point-detector locations showed the trend expected from the explicit modeling of the discrete CsCl capsules. The rigor in the SAS4 treatment of the physics of gamma photon attenuation in materials has its attendant cost, which is largely time spent in learning the appropriate use of the specific SAS4 procedures by the first author. However, the experience was directly beneficial during the three-dimensional Monte Carlo analysis of gamma radiation streaming from the drain ports of the BUSS cask, which is a much more challenging task computationally than calculating dose rates on the general body of the cask.

ACKNOWLEDGMENT

The authors would like to thank Judy Fisher for her excellent desk-top integration of graphics and text in this paper.

REFERENCES

Beneficial Uses Shipping System (BUSS) Cask Safety Analysis Report for Packaging (SARP), Vols. I and II, Sandia National Laboratories, Rev. 3 (1991)

Liu, Y. Y., et al. *Monte Carlo Validation of Gamma Radiation Streaming from a Radioactive Material Shipping Cask,* to be published in Proc. Topical Meeting on Radiation Protection and Shielding, April 1996

MICROSHIELD User's Manual, A Program for Analyzing Gamma Radiation Shielding, Version 3.12, Grove Engineering, Inc., Washington Grove, MD (1988)

Robins, D. Westinghouse Hanford Co., *personal communication* (1994)

SCALE: A Modular Code System for Performing Standardized Computer Analyses for Licensing Evaluation, NUREG/CR-0200, Vols. 1-4, Rev. 4, ORNL/NUREG/CSD-2/R4 (1995)

Tang, J. S. *SAS4: A Monte Carlo Cask Shielding Analysis Module Using an Automated Biasing Procedure,* NUREG/CR-0200, Vol. 1, Sec. S4, Rev. 4, ORNL/NUREG/CSD-2/V2/R4 (1993)

West, J. T. and Emmett, M. B. *MARS: A Multiple Array System Using Combinatorial Geometry,* NUREG/CR-0200, Rev. 4, Vol. 3, Sec. M9, ORNL/NUREG/CSD-2/V3/R4 (1995)

Yoshimura, H. R., et al. *The Beneficial Uses Shipping System Cask,* PATRAM '86, Davos, Switzerland p. 81 (1986)